Study of the discovery potential for an invisibly decaying Higgs boson via the associated ZH production in the ATLAS experiment

Frank Meisel,
M. Dührssen, M. Heldmann and K. Jakobs
University of Freiburg, Germany

6th March 2006

Abstract

The decay of a Higgs boson into invisible particles is well motivated in many extensions of the Standard Model. In this note an evaluation of the discovery potential of the ATLAS experiment for an invisibly decaying Higgs boson, produced in association with a Z boson, is discussed. In particular, the uncertainties related to the normalization of the dominant backgrounds are addressed.

1 Introduction

One of the main physics goals of the experiments at the LHC is the discovery of the mechanism responsible for electroweak symmetry breaking. It has been demonstrated in many studies over the past years [1, 2] that a Standard Model Higgs boson can be discovered with a high signal significance. However, a discovery of a Higgs boson which has a significant branching ratio into invisible final states is more difficult. Within the Standard Model no invisible decay modes appear and an observation of a Higgs boson with decays into invisible final states would be an indication of physics beyond the Standard Model. In the minimal supersymmetric extension of the Standard Model (MSSM) Higgs bosons can decay, in some regions of the parameter space, with a large branching ratio into the lightest neutralino or gravitinos [3, 4]. In models with an enlarged symmetry breaking sector, Higgs bosons can decay into light weakly interacting scalars [5, 6, 7]. Invisible Higgs boson decays can also appear in models with large extra dimensions [8, 9] or if massive neutrinos of a fourth generation exist [10].

Searches for invisibly decaying Higgs bosons have been performed at the e^+e^- collider LEP in the ZH associated production mode [11]. Since no evidence for an invisibly decaying Higgs boson has been found, a lower limit on its mass of 114.4 GeV/c^2 has been placed, assuming Standard Model couplings in the production and a branching ratio into invisible final states of 100% ($BR(H \rightarrow \text{inv}) = 1$) [11]. Although a large fraction of the SUSY parameter space with invisible Higgs decays is excluded in the constrained MSSM (given the mass limits on the lightest neutralino from LEP experiments), invisible decays could be enhanced if gaugino mass unification is abandoned [4].

At a hadron collider, triggering and detection of invisible final states is only possible if the Higgs boson is produced in association with other particles. Higgs bosons can be searched for in the associated production modes with vector bosons (WH, ZH), $t\bar{t}$-pairs ($t\bar{t}H$) and jets (vector boson fusion mode qqH). All three processes have already been suggested in the literature and feasibility studies have been performed [12, 13, 14, 15]. In all cases missing transverse energy is used as a key signature for the presence of an invisible Higgs boson decay. More detailed simulations including the performance of the ATLAS experiment have been carried out for the vector boson fusion mode [16], for the associated $t\bar{t}H$ [17] and for the WH and ZH production modes [18].

In this note, the search for an invisibly decaying Higgs boson in the ZH production mode is re-assessed. Since a signal can only be extracted from an excess of events with large missing transverse momentum above the background from known processes, the absolute knowledge of these backgrounds is important to establish a signal. In the present study it has been estimated how well those backgrounds can be constrained and determined from a direct measurements of related channels in the ATLAS experiment. It must be stressed that so far only Standard Model backgrounds have been considered. An investigation of a more realistic scenario where, as an example, invisibly decaying Higgs bosons are studied in a SUSY scenario including backgrounds from SUSY processes, is currently being performed [19]. Since it has already been shown in Refs. [18, 20] that due to the overwhelming background from inclusive W production a signal cannot be extracted in the WH production mode only the ZH mode is considered.

In Section 2, the signal properties and the background processes are discussed, before the event selection is presented in Section 3. A detailed discussion of the systematic uncertainties and of the normalization of the major backgrounds is presented in Section 4. Finally, the determination of the signal significance is given in Section 5, before a comparison to other channels is presented in Section 6.

2 Signal and Backgrounds

At the LHC the dominant Higgs boson production process is gluon fusion. The associated ZH production has a cross section which is about a factor of 30 lower than the gluon-fusion cross section and only plays a minor role in the search for a Higgs boson in the standard decay modes. However, due to the accompanying Z boson, which can be well reconstructed in its leptonic decay modes, $Z \rightarrow \ell\ell$, it is important in the search for invisible decays. To establish the nature of an invisibly decaying particle, it is of utmost importance to combine the information from several channels. Therefore this channel complements the search in the $t\bar{t}H$ and qqH modes.

m_H	(GeV/c^2)	120	140	160	180	200	300	400
$\sigma(ZH)$	(fb)	744	458	295	199	137	31	10.0
$\sigma(ZH) \cdot BR(Z \to \ell\ell)$	(fb)	49.9	30.7	19.8	13.4	9.20	2.08	0.67

Table 1: *Leading order ZH production cross sections and $\sigma \cdot BR(H \to inv = 100\%) \cdot BR(Z \to \ell\ell)$ with $\ell = e, \mu$ as a function of the Higgs boson mass. The cross sections have been computed using the program* h2hv *of Ref. [21].*

The signal process considered

$$pp \;\to\; ZH \;\to\; \ell\ell \; \not{p}_T \qquad\qquad \text{with} \;\; (\ell = \mathrm{e}, \mu)$$

results in a final state with two isolated high p_T leptons from the Z-boson decay and large missing transverse momentum from the Higgs-boson decay. This final state can easily be triggered using the standard ATLAS trigger menus. This is a clear advantage compared to the vector boson fusion mode [16]. The signal cross sections times the leptonic branching ratios ($Z \to \ell\ell, \ell = e, \mu$) are given for Higgs boson masses in the range between 120 and 400 GeV/c^2 in Table 1. The cross sections have been calculated using the program h2hv [21] which uses the CTEQ5L parametrization [22] of the parton density functions. They agree with the values given in Ref. [23]. For the Higgs boson decays into invisible particles a branching ratio of 100% is assumed in the following.

The event simulation has been performed using the PYTHIA Monte Carlo program [24], including parton showering and hadronization. The detector simulation has been carried out using ATLFAST [25], the fast simulation package of the ATLAS detector, which has been implemented in the ATHENA 7.0.3 framework.

As an example of a kinematic distribution, the transverse momentum of the Higgs boson, which results in the missing transverse momentum in signal events, is shown in Fig. 1 for various Higgs boson masses.

The principle backgrounds result from di-boson, $t\bar{t}$ and Z+jet production. The following processes have been considered:

- ZZ, with $ZZ \to \ell\ell\nu\nu$
  This process constitutes an irreducible background since the final state topology is identical to the one of the signal. Despite the relatively small production cross section it constitutes a significant background after the selection cuts have been applied.

- WZ, with $Z \to \ell\ell$ and $W \to \ell\nu$ or $W \to \tau\nu_\tau$
  This background contributes when the lepton originating from the W is not identified. Additional contributions result from W decays into taus which subsequently decay hadronically.

- $WW \to \ell\nu\ell\nu$
  Although this process constitutes an irreducible background, it can be efficienctly suppressed by applying a cut on the invariant mass of the two leptons.

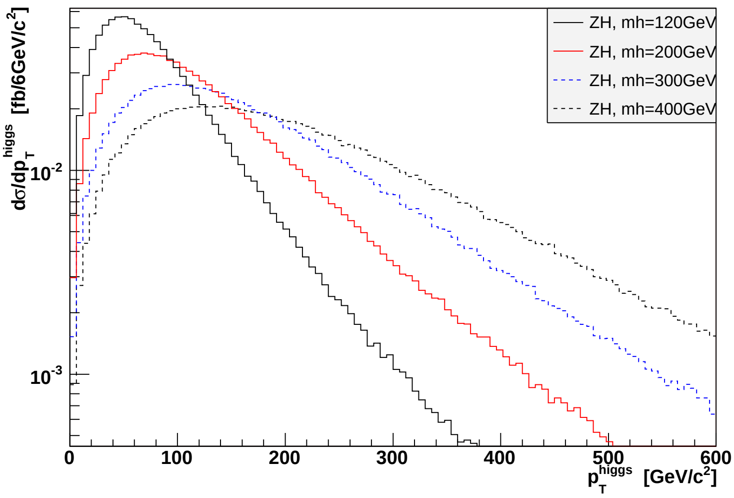

Figure 1: *Transverse momentum of the Higgs boson, which at parton level is identical to the missing transverse momentum, for different Higgs boson masses (at parton level).*

- $t\bar{t} \rightarrow WWb\bar{b} \ \rightarrow \ell\nu\ell\nu b\bar{b}$
  This background contributes via the leptonic decays of the top quarks. Due to the large production cross section it is expected to contribute significantly, despite large rejection factors.

- Inclusive Z production
  Like in the $t\bar{t}$ case, inclusive Z production may contribute due to its large production cross section. A significant contribution is either expected from high mass off-shell $Z \rightarrow \tau\tau$ decays when both taus decay leptonically or from high mass off-shell, high η $Z(\rightarrow \ell\ell)$ decays with high p_T leptons. Other contributions may result from $Zb\bar{b}$ production.

The production cross sections for all background processes are summarized in Table 2. It should be noted that no leptonic decays have been forced in the simulation and inclusive cross sections are given.

3 Selection Cuts

In order to separate the signal process from the large backgrounds the following cuts have been applied:

1. Trigger
   The di-lepton triggers can be used to select the events at trigger level. Events are kept

process	cross-section (pb)	Number of events generated
ZZ	11.1	15 Mio
WZ	26.8	5 Mio
WW	70.1	5 Mio
$t\bar{t}$	490	300 Mio
Z ($p_T(Z) > 60$ GeV/c)	591000	100 Mio

Table 2: *Cross sections of relevant background processes (no leptonic branching ratios included). The cross sections have been calculated using leading order matrix elements in the PYTHIA Monte Carlo program.*

if two electrons with p_T >15 GeV/c within $|\eta|$ <2.5 or two muons with p_T >10 GeV/c within $|\eta|$ <2.4 are found in the final state.[1]

2. Two Leptons
   It is required that there are exactly two identified isolated leptons with $p_T > 15$ GeV/c (for electrons) and $p_T > 10$ GeV/c (for muons) within the pseudorapidity range $|\eta| < 2.5$. Events where a third lepton with $p_T > 7$ GeV/c is identified are rejected. An identification efficiency of 90% per lepton is assumed.

3. Id + Charge
   The two leptons are required to have the same flavour and opposite charge.

4. Z-Mass
   The invariant mass of the leptons is required to be in the range of $m_Z \pm 10$ GeV/c^2.

5. Missing transverse momentum, $\not{p}_T$
   For a good separation between signal and backgrounds the missing transverse momentum is required to exceed 100 GeV/c.

6. Jet Veto
   In order to reject the large $t\bar{t}$ background, a veto on the hadronic activity is applied and events containing a jet with $p_T > 30$ GeV/c and within $|\eta| < 4.9$ are rejected. The rather high value of 30 GeV/c has been chosen to avoid large systematic uncertainties.

7. b-jet Veto
   In addition, events which contain a tagged b-jet with a p_T value above the b-jet identification threshold of 15 GeV/c are rejected. This veto increases significantly the rejection against $t\bar{t}$ events. A b-tagging efficiency of 60% with the corresponding rejection factors of 100 against light and 10 against c-jets has been assumed.

[1] We are aware that some pickup is possible via single lepton triggers, which are set by a high p_T leading lepton and where a second lepton is below the threshold of the di-lepton triggers. Those contributions are small and have been neglected.

8. Transverse Mass
   The transverse mass of the di-lepton-$\not p_T$ system, defined as

$$m_T \;=\; \sqrt{2 p_T^{\ell\ell}\; \not p_T \;(1 - \cos\Delta\phi)},$$

   where $\Delta\phi$ represents the azimuthal separation between the di-lepton system and the missing transverse momentum vector, is used to further separate signal and background. The cut $m_T > 200$ GeV/c^2 is applied.

The motivation for the application of these cuts can be seen from Fig. 2, where the distributions of the di-lepton invariant mass, the missing transverse momentum, the number of reconstructed jets with p_T >30 GeV/c and the transverse mass m_T are shown before the relevant cuts are applied.

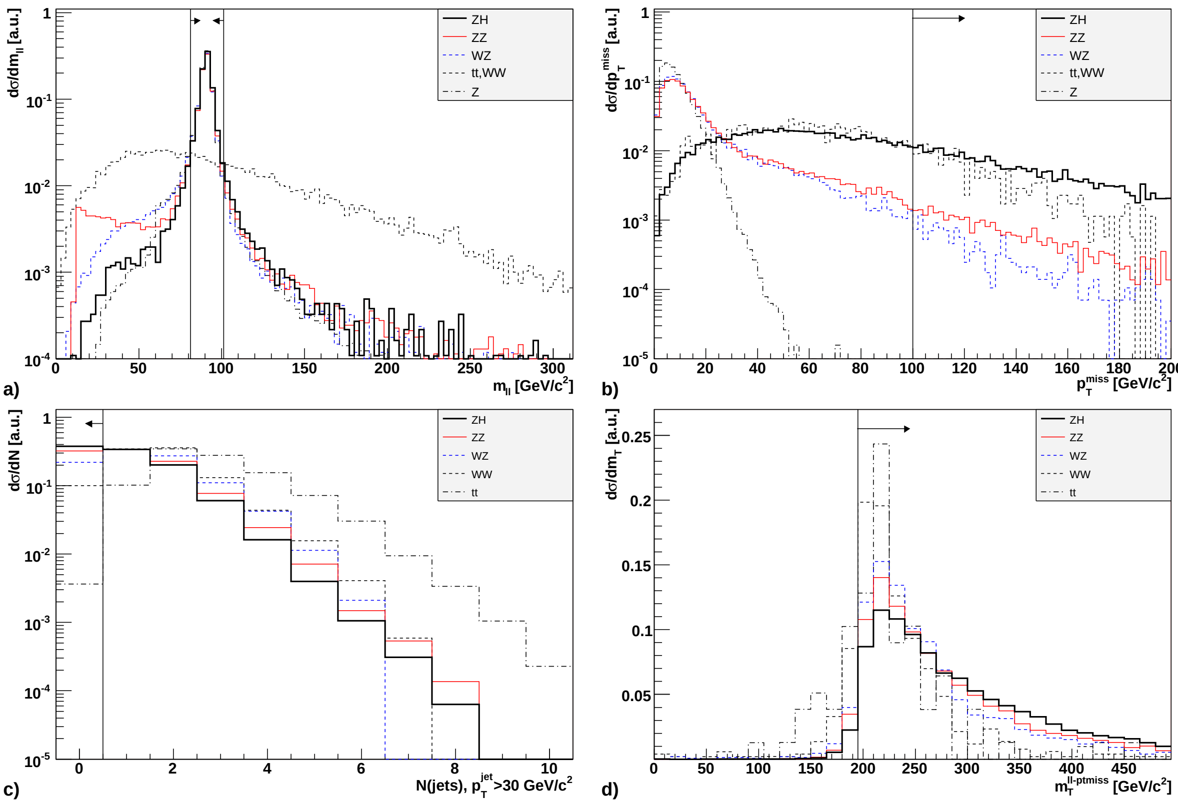

Figure 2: *The distributions of a) the di-lepton invariant mass, b) missing transverse momentum, c) number of reconstructed jets with p_T > 30 GeV/c and d) transverse mass m_T for a Higgs boson signal with m_h=120 GeV/c^2 and for the various backgrounds before the relevant cuts are applied. All distributions are normalized to unity.*

The accepted cross sections after applying the consecutive cuts are given in Table 3 for a Higgs boson with a mass of 120 GeV/c^2 and for the various backgrounds. For the

σ [fb]	Signal	ZZ	WZ	WW	$t\bar{t}$	Z	$\sum$ Bg
Cut0:	744	1.1 E4	2.7 E4	7.0 E4	4.9 E6	5.9 E8	5.9 E8
Cut1:	27.7	784	1.0 E3	1.8 E3	1.8 E4	1.6 E4	1.6 E4
Cut2:	22.4	615	726	1.4 E3	1.4 E4	1.2 E6	1.2 E6
Cut3:	22.2	602	627	718	6.8 E3	1.2 E6	1.2 E6
Cut4:	19.8	502	531	94.0	915	9.4 E5	9.4 E5
Cut5:	6.01	15.8	7.86	1.43	162	5.39	192
Cut6:	4.47	11.6	4.42	0.93	0.90	0.08	17.9
Cut7:	4.40	11.3	4.34	0.92	0.66	0.08	17.3
Cut8:	4.21	10.7	3.97	0.77	0.31	< 0.03	15.78

Table 3: *Accepted cross sections after applying cuts 1–8 (see text) for a Higgs boson signal with m_H = 120 GeV/c^2 and the various backgrounds.*

Higgs boson, the Standard Model production cross section and a totally invisible decay (BR (H $\rightarrow$ inv) = 1) have been assumed. After all cuts a signal cross section of 4.21 fb is expected. The residual background is dominated by the di-boson production, which sums up to 15.4 fb, of which 69% are taken by the irreducible $ZZ \rightarrow \ell\ell\nu\nu$ background. The reducible backgrounds can be strongly suppressed by the selection cuts. The dominant contribution is given by the $t\bar{t}$ background, which corresponds to an accepted cross section of 0.3 fb. The dominant contribution (88%) of the remaining Z-inclusive sample originates from $Z \rightarrow \mu\mu$ events with high mass (~500 GeV/c^2-1 TeV/c^2) for which the degraded resolution for high p_T muons leads to significant p_T^{miss}. The remaining 12 % are due to $Z \rightarrow \tau\tau \rightarrow \ell\ell$ events. Both types of events show a flat invariant mass distribution to high m_Z values so that the estimation can be done as for the $t\bar{t}$ and WW estimation, as described in the following Section.
The signal-to-background ratio reaches about 1:4, however, it must be stressed again that no mass peak can be reconstructed and a signal claim is entirely based on an excess of events above the background.

Finally, the accepted signal cross section has been computed as a function of the Higgs boson mass. The corresponding results are given in Table 4 for masses in the range between 120 and 400 GeV/c^2. Over this mass range the signal-to-background ratio varies between 26% (for m_H =120 GeV/c^2) and 1.3% (for m_H =400 GeV/c^2). The limiting factor for large Higgs boson masses is the small signal production cross section.

m_H (GeV/c^2)	120	140	160	180	200	300	400
Cut 0	744	458	295	199	137	31	10.0
Cut 1: Trigger	27.7	18.0	11.6	7.90	5.61	1.24	0.37
Cut 2: 2 Leptons	22.4	14.5	9.42	6.39	4.54	1.00	0.30
Cut 3: Flavour+Charge	22.2	14.4	9.32	6.31	4.48	0.99	0.29
Cut 4: Z Mass	19.8	12.9	8.35	5.66	3.98	0.84	0.24
Cut 5: $\not{P}_T$	6.01	4.83	3.61	2.70	2.25	0.51	0.12
Cut 6: jet Veto	4.47	3.48	2.57	1.91	1.45	0.34	0.08
Cut 7: b-jet Veto	4.40	3.42	2.53	1.88	1.42	0.34	0.08
Cut 8: Transvers mass	4.21	3.29	2.45	1.83	1.39	0.33	0.07

Table 4: *Accepted cross sections after applying cuts 1–8 (see text) for various Higgs boson masses in the range between 120 and 400 GeV/c^2.*

4 Normalization of the backgrounds

An estimate of the major backgrounds from ZZ and WZ production can be obtained in the ATLAS experiment using control samples from the data itself. Therefore an absolute theoretical prediction, which is usually affected by large uncertainties, is not needed. The method and an estimate of the uncertainties is discussed in the following.

4.1 Normalization of the ZZ background

The $ZZ \rightarrow \ell\ell\nu\nu$ background can be determined from a measurement of $ZZ \rightarrow \ell\ell\ell\ell$ decays. Applying cuts which are similar to the ones applied in the invisible Higgs boson signal selection, the background in the four lepton channel is expected to be very small. This is supported by the studies performed for the ATLAS physics TDR [1] on the $H \rightarrow ZZ \rightarrow 4\ell$ search. In final states with two on-shell Z bosons, no other background than the continuum ZZ production, which represents the signal in this analysis, was identified.

If such a normalization channel is used, it is important to understand any acceptance differences which might deteriorate the naively expected difference in rate between the two channels resulting from different branching ratios. In the present case, it is expected that the two channels differ by a factor $R = \mathrm{BR(ZZ} \rightarrow \ell\ell\nu\nu)/\mathrm{BR(ZZ} \rightarrow \ell\ell\ell\ell) = 2 \cdot \mathrm{BR(Z} \rightarrow \nu\nu)/\mathrm{BR(Z} \rightarrow \ell\ell)$. If only two charged lepton flavours (e, μ) are taken into account, this ratio is expected to be 5.98. A first correction to this number results from $Z \rightarrow \tau\tau$ contributions, which are expected to slightly decrease the ratio due to $\tau \rightarrow \ell\nu\nu$ decays. However, the p_T spectrum of leptons resulting from tau decays is expected to be soft and the invariant $\ell\ell$ mass is not consistent with the Z mass.

A comparison of the accepted cross sections for the $2\ell - \not{p}_T$ and 4ℓ searches is presented in Table 5. It is assumed that in both cases only ZZ production contributes to the final sample. The numbers have been extracted from a high statistics Monte Carlo simulation of ZZ production including γ^* and Z^* contributions.

In the upper part of the Table numbers are given, as they would be measured by applying an experimental selection procedure. In order to separate the contributions from $Z \rightarrow \tau\tau$ decays, two numbers are given for each cut in the Table. The numbers in brackets correspond to the case where τ contributions have been neglected. The following cuts have been applied:

- Trigger cuts: either two electrons with $p_T >$15 GeV/c within $|\eta| < 2.5$ or two muons with $p_T >$10 GeV/c within $|\eta| < 2.4$ are required.

- Lepton cuts: Two identified isolated electrons with $p_T >$15 GeV/c or two identified isolated muons with $p_T >$10 GeV/c within $|\eta| < 2.5$. In the 4ℓ selection two additional leptons with $p_T > 7$ GeV/c within $|\eta| <$2.5 are required. The lepton identification efficiency is assumed to be 90% per lepton.

- It is required that one respectively two on-shell Z bosons are reconstructed, *i.e.,* there should be one/two pairs of same flavour and opposite-sign leptons with 80 GeV/c^2

	No cuts	Trigger cuts	Lepton cuts	Z-Mass cuts	$\not{p}_T >$ 100 GeV/c^2	Jet vetos	$m_T >$ 200 GeV/c^2	Relaxed cuts
σ_{acc} (fb)	11092	784	602	502	15.8	11.3	10.7±0.1 stat.	67.6
$ZZ \to \ell\ell\nu\nu$ search	(10239)	(735)	(573)	(483)	(15.4)	(11.2)	(10.5)	(64.7)
σ_{acc} (fb)	11092	784	12.0	8.09	1.27	0.92	0.85±0.02stat.	4.95±0.05 stat.
$ZZ \to 4\ell$ search	(10239)	(735)	(11.7)	(8.07)	(1.26)	(0.90)	(0.85±0.02 stat.)	(4.94±0.05 stat.)
Ratio		1	50	60	12.4	12.3	12.6±0.3 stat.	13.6±0.15 stat.
Ratio (no $Z \to \tau\tau$)		(1)	(48)	(60)	(12.2)	(12.4)	(12.4±0.3 stat.)	(13.2±0.15 stat.)
Lepton cuts applied to neutrinos (parton level):								
σ_{acc} (fb)	11092	778	62.4	48.7	7.69	5.66	5.36±0.05 stat.	29.8
$ZZ \to \ell\ell\nu\nu$ search	(10239)	(735)	(61.2)	(48.7)	(7.69)	(5.66)	5.36±0.05 stat.	(29.67)
σ_{acc} (fb)	11092	784	12.0	8.09	1.27	0.92	0.85±0.02 stat.	4.95±0.05 stat.
$ZZ \to 4\ell$ search	(10239)	(735)	(11.7)	(8.07)	(1.26)	(0.90)	(0.85±0.02 stat.)	(4.94±0.05 stat.)
Ratio (exp.:5.98)		1	5.20	6.02	6.05	6.12	**6.27±0.16 stat.**	**6.02±0.06 stat.**
Ratio (no $Z \to \tau\tau$)		(1)	(5.22)	(6.02)	(6.11)	(6.27)	(6.32±0.16 stat.)	(6.03±0.06 stat.)

Table 5: *Accepted cross sections for the $ZZ \to 4\ell$ and $ZZ \to \ell\ell\nu\nu$ selections.*

$< m_{\ell\ell} <$100 GeV/c^2. If more than one combination is possible, the one is chosen that minimizes the χ^2 value: $\chi^2 = (m_{Z_1} - m_Z)^2 + (m_{Z_2} - m_Z)^2$. At this stage, the dilepton trigger cut on the remaining $Z \to \ell\ell$ — which will not be treated as the fake $Z \to \nu\nu$ — is applied again.

- A cut on the missing transverse momentum needs to be applied to select $\ell\ell\nu\nu$ final states. Since additional leptons have already been required in the 4ℓ selection, it is required that the $\not{p}_T$ corrected by the p_T of one of the two Z bosons -chosen randomly- passes this cut, *i.e.*, two leptons are treated as neutrinos.

- Jet veto and m_T cuts: finally the jet veto cuts and the cut on the transverse mass as discussed in Section 3 are applied.

After applying the $\not{p}_T$ and the jet veto cuts, one obtains an accepted cross section of 0.85 fb and a normalization factor of 12.58±0.32 between the two channels. As can be seen from the numbers in brackets, the $Z \to \tau\tau$ contributions are small after final cuts. Their contributions to the 4ℓ channel are already negligible after the Z mass cut is applied. In the $\ell\ell\nu\nu$ case, they still contribute via $ZZ \to \ell\ell\tau\tau$ decays. However, the dominant contributions from hadronic τ decay modes are largely suppressed after jet veto cuts. The ratio found between the two channels is about a factor of two larger than the expectation from the branching ratios. This is mainly due to acceptance and efficiency factors for the two additional leptons in the 4ℓ channel.

An attempt has been made to trace back the differences by using parton level information. The results are given in the lower part of Table 5. In this study the selection has been modified such that the neutrinos from the $Z \to \nu\nu$ decays in the $\ell\ell\not{p}_T$ selection are treated as charged leptons and are subjected to the lepton identification criteria.[2] In

[2]The effect of the magnetic field has been proven to be negligible for the relevant cut variables for the leptons.

order to account for the lepton isolation the standard ATLFAST lepton isolation algorithm for muons has been applied to neutrinos. To treat leptons and neutrinos consistently, an additional efficiency correction is necessary. In the ATLFAST algorithm there are differences in the treatment of electrons and muons which result in slightly different isolation efficiencies. For electrons, energy depositions which are found in a narrow cone of $\Delta R < 0.15$ around the true electron direction may be added to the electron cluster. If added to the cluster, this energy is no longer added to the isolation energy sum which is computed in a larger cone of $\Delta R < 0.4$ and is used to define the lepton energy isolation. For muons -which do not leave a cluster in the ATLAS calorimeters- all such energies are considered in the isolation energy sum. The isolation efficiencies for various ZZ final states as found in ATLFAST using the standard isolation criteria, normalized to true leptons with $p_T > 6$ GeV/c within $|\eta| < 2.5$ are given in Table 6.

	Lepton isolation efficiencies ϵ [%]				
	$ZZ \to 4\ell$ sample		$ZZ \to \ell\ell\nu\nu$ sample		Correction factor
	$\mu\mu\mu\mu$	69.1			0.907
FSR ON	$\mu\mu ee$	71.5	$\ell\ell\nu\nu$	76.2	0.938
	$eeee$	73.8			0.969
	$\mu\mu\mu\mu$	81.4			0.961
FSR OFF	$\mu\mu ee$	88.3	$\ell\ell\nu\nu$	84.7	1.043
	$eeee$	95.1			1.123

Table 6: *Lepton isolation efficiencies per event for different ZZ final states.*

In addition to the lepton flavours the isolation efficiencies are found to depend on final state radiation (FSR). Numbers are given for both cases, FSR taken into account and FSR switched off. Photon radiation leads to a lower isolation efficiency for all leptons. From the numbers in the table an electron isolation efficiency of 92.7% (98.8%) can be deduced if final state radiation is switched on (off). The corresponding numbers for muons are 91.2% and 95.0%. If final state radiation is switched off, the isolation efficencies for muons and neutrinos are found to be equal. The efficency corrections, *i.e.*, the ratio between the efficiency measured in the 4ℓ and in the $\ell\ell\nu\nu$ channel, for the different four lepton final states are also given in Table 6.

In addition to the isolation efficiency, a global neutrino identification efficiency factor of $(0.9)^2$ is applied to treat charged leptons and neutrinos equally. The invariant Z mass cut in the $\ell\ell \not{p}_T$ selection is applied to both the di-lepton and the di-neutrino system. A small difference results from final state photon radiation off leptons. In ATLFAST this radiation is not added to the electron energy and therefore leads to a small shift of the Z mass peak to lower invariant di-lepton masses. However, this effect is negligible, once the photon energy is added to the calorimeter cluster energy, as would be done in an electron reconstruction algorithm.

Due to contributions from γ^*/Z production and interference the lineshapes are expected to be different for di-lepton and di-neutrino final states. These differences are, however, small after the invariant mass cut of ± 10 GeV/c^2 around m_Z has been applied. After accounting for the various efficiency differences, the expected ratio between the 4ℓ and the $\ell\ell\nu\nu$ channel is confirmed, as can be seen from the numbers given in the last row of Table 5.

The final accuracy of the ZZ background normalization is limited by the statistical error on the number of $ZZ \to 4\ell$ events. In order to reduce this error, the m_T cut has not been applied and the cut on $\not{p}_T$ has been relaxed to 30 GeV/c. If those relaxed cuts are applied the accepted cross section rises by a factor of about six and reaches 4.95 fb. The final background normalization factor R_{ZZ} which has to be applied as a scale factor to the measured $ZZ \to 4\ell$ rate is given by:

$$\begin{aligned} R_{ZZ} &= 2 \cdot \frac{BR(Z \to \nu\nu)}{BR(Z \to \ell\ell)} \cdot \xi_\tau \cdot \xi_{lept} \\ &= 5.98 \cdot 1.043 \cdot 2.190 = 13.65, \end{aligned}$$

where the correction factors ξ can be determined from the numbers given in Table 5. Also these correction factors are affected by systematic uncertainties. Those are largest for the factor ξ_{lept} which accounts for differences in the identification, acceptance and isolation of leptons as compared to neutrinos. In the following it is assumed that the uncertainty on the Monte Carlo determination of this factor is $\pm 2\%$. This should include uncertainties in the lepton identification efficiency, which does not cancel in the ratio R_{ZZ}. The uncertainties on the factor ξ_τ are less important, since the corrections are small.

Since relaxing the $\not{p}_T$ and m_T cuts changes the selected ZZ phase space, it is important to investigate how the di-boson spectra are affected. In Fig. 3, the p_T and η distributions of the parton ZZ system are shown for the two cut scenarios assuming a data sample of 100 fb^{-1}. The distributions show that the statistical error which is indicated by the shaded region dominates the differences between the shapes. Within this error both curves show good agreement. It is expected that at the time when this analysis is going to be performed, ZZ production has been measured with such an accuracy that an extrapolation from the relaxed to the hard cuts can be done with an uncertainty at the few percent level.

It should be noted that all studies on the differences between the two selections discussed above have been performed using the fast simulation ATLFAST. The numbers found here, in particular for the efficiency differences, will not hold for real data or for full simulation. However, the study indicates that subtle differences need also to be dealt with in the future to obtain a proper normalization.

If data corresponding to an integrated luminosity of 30 fb^{-1} are collected, 148 $Z \to 4\ell$ events are expected to be measured. This results in a systematic uncertainty of $\pm 8.5\%$ for the $ZZ \to \ell\ell\nu\nu$ background. For an integrated luminosity of 100 fb^{-1}, the corresponding uncertainty would be $\pm 4.9\%$.

4.2 Normalization of the WZ background

Also the second largest background, resulting from WZ production, can be normalized from data. A detailed Monte Carlo analysis has shown that this background has three major contributions:

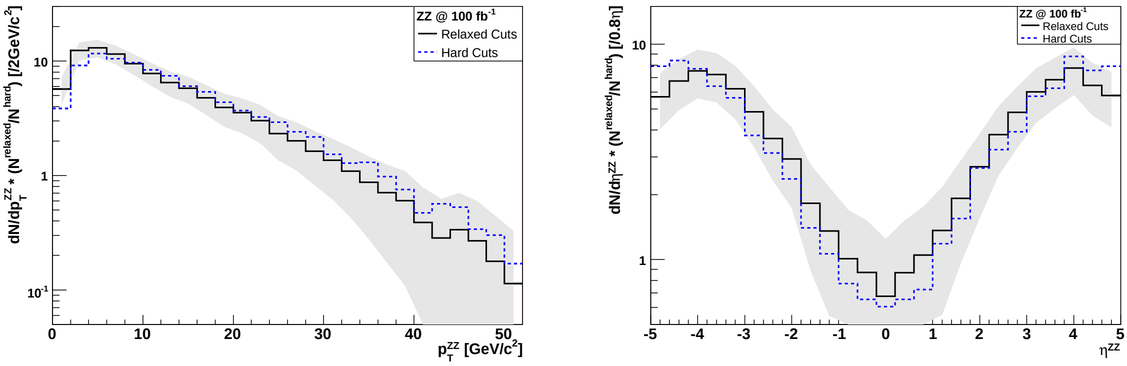

Figure 3: *Left: The p_T distribution of the ZZ system on parton level after applying relaxed and hard cuts. The shaded area corresponds to the statistical uncertainty for an integrated luminosity of 100fb^{-1}. Right: The η distribution of the ZZ system. In both figures the distributions for hard cuts are normalized to those for the relaxed cuts (N^{rel}/N^{hard}).*

- $W \to e\nu_e$ events contribute to the $\not{p}_T$ signature if the lepton from the W decay is lost, *i.e.*, it is either not identified or is outside the lepton acceptance $|\eta|$ >2.5.
- $W \to \mu\nu_\mu$ events contribute in principle in the same way as $W \to e\nu$ events with the muon being either not identified or outside the acceptance. Since there is no muon detection beyond $|\eta| < 2.5$ the muon contributes in addition to the total missing transverse momentum.
- $W \to \tau\nu_\tau$ events, with both leptonic and hadronic decays of the W, represent the largest background contribution. The lepton p_T spectrum from the leptonic decays is softer than that from direct W decays and the probability that the lepton is not identified in the central region $|\eta| < 2.5$ is larger (below p_T threshold). The largest contribution results, however, from hadronic tau decays. If the decay products are in the pseudorapidity region $|\eta| < 2.5$ such events would only be rejected if the p_T of the hadronic tau would exceed the jet veto p_T threshold of 30 GeV/c.

The total WZ background with an accepted cross section after final cuts of 3.92 fb has been broken down into the various contributions and the corresponding numbers are given in Table 7. The $W \to \tau\nu$ fraction represents about 54% of the background, of which about 75% have τ decay products in the acceptance region $|\eta| < 2.5$.

In order to normalize the WZ background three-lepton final states can be used. In the event selection a third lepton with $p_T > 10$ GeV/c is required, *i.e.*, the veto on a third lepton is reversed. In case of three leptons with the same flavour, the lepton pair (out of three combinations) having an invariant mass closest to m_Z is considered as coming from the Z boson. The accepted cross sections for the standard two-lepton and for the three-lepton searches are given in Table 8.

W decay mode	σ (fb)		fraction	
	all	$\|\eta\|$ <2.5 $p_T > 10$ GeV/c	all	$\|\eta\|$ <2.5 $p_T > 10$ GeV/c
$W \to e\nu$	0.49	0.12	12.3%	3.0%
$W \to \mu\nu$	1.33	0.25	33.5%	6.3%
$W \to \tau\nu$	2.15	1.42	54.2%	35.8%
$\to e\nu\nu\ \nu$	0.36	0.23	9.1%	5.8%
$\to \mu\nu\nu\ \nu$	0.44	0.24	11.0%	6.0%
$\to had.\nu\ \nu$	1.35	0.95	34.0%	23.9%

Table 7: *The contribution of the WZ background, broken down into the various W and τ decay modes (see text).*

	No cuts	Trigger cuts	Lepton cuts	Z mass cuts	$\not{p}_T > 100$ GeV/c	Jet vetos	m_T cut	$\not{p}_T$ and m_T relaxed
σ_{acc} (fb) $WZ \to \ell\ell$ search	26770	1013	627	531	7.9	4.34	3.97	23.9
σ_{acc} (fb) $WZ \to \ell\ell\ell$ search	26770	1013	110	93.7	5.7	4.14	3.83	29.4
σ_{acc} (fb) $ZZ \to \ell\ell\ell$ search	11092	783	20.28	16.4	0.2	0.09	0.06	1.3
σ_{acc} (fb) $t\bar{t} \to \ell\ell\ell$ search	490000	17930	162	23.2	3.5	0.07	0.07	1.3

Table 8: *Accepted cross sections for the $WZ \to \ell\ell$ and $WZ \to \ell\ell\ell$ selections.*

The selected three lepton sample is expected to be dominated by genuine WZ production with only small contributions from ZZ and $t\bar{t}$ production. These three lepton events can be used to estimate with a relatively small uncertainty that fraction of the WZ background for which the third lepton with $p_T > 10$ GeV/c is within $|\eta| < 2.5$ (being either undetected or a hadronic τ).

It has been investigated how well the p_T of the reconstructed third identified lepton agrees with the p_T of the τ lepton (at parton level) resulting from a $W \to \tau\nu$ decay. In Fig. 4(left) the shapes of the p_T distributions are compared. Since both distributions agree well, a reliable background normalization can be made. In order to increase the statistical power of the normalization sample the m_T can be dropped and the $\not{p}_T$ cut can be relaxed. The compatibility of the shapes of the p_T spectra has been investigated as a function of the $\not{p}_T$ cut. In Fig. 4(right) the χ^2 probability for the agreement of the two spectra is given as a function of the $\not{p}_T$ cut. This study suggests that the spectrum remains unbiased for a $\not{p}_T$ cut above ~50 GeV/c (within the statistical uncertainties for a data set corresponding to an integrated luminosity of 30 fb^{-1}). However, as shown in Table 8 the fraction of the ZZ and $t\bar{t}$ background increases from 3.3 to 8.1% if the m_T is dropped and the $\not{p}_T$ cut is lowered from 100 to 50 GeV/c.

Applying the three lepton selection, a total WZ cross section of 29.4 fb is expected. Like for the ZZ background, Monte Carlo calculations are used to determine the ratio between the three-lepton normalization channel and the background component. This ratio has been found to be $R_{WZ} = 0.81 \pm 0.03$. As before, a systematic error of ±2% on the lepton identification efficiency has been assumed.

The WZ background contributions with the lepton in the region $|\eta| > 2.5$ can be estimated by extrapolating the shape of the pseudorapidity distribution beyond the tracking region. It is assumed that the pseudorapidity distribution can be well modelled using Monte Carlo simulation [26]. To be conservative, a 10% systematic error has been assumed.

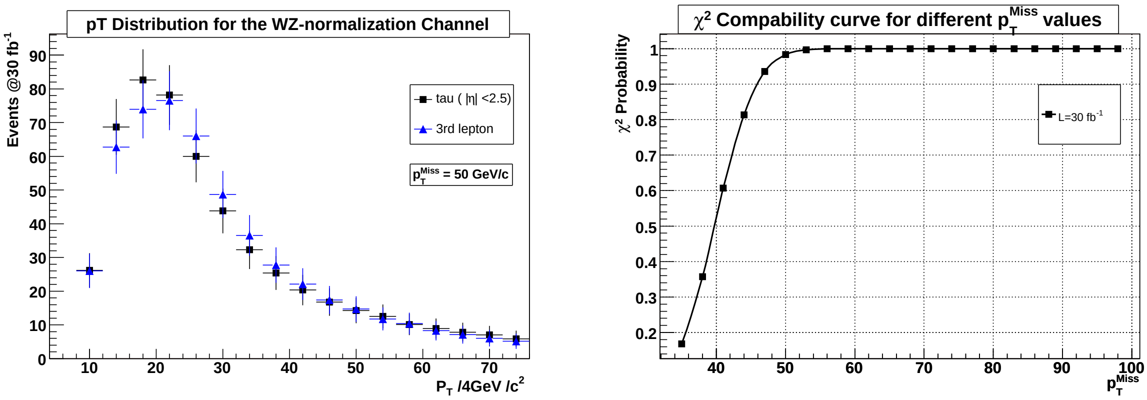

Figure 4: *Left: Comparison of the p_T distributions of the third lepton of the $WZ \to \ell\nu\ell\ell$ normalization channel and the $WZ \to \tau\nu\ell\ell$ background channel (parton level information is used for the τ), where the τ is within the pseudorapidity range $|\eta| <2.5$. Right: The χ^2 probability for the compatibility of the p_T distribution as a function of the $\not{p}_T$ cut.*

Based on the estimated cross sections for the three lepton events, the WZ background with a third lepton with $p_T > 10$ GeV/c in the region $|\eta| < 2.5$ can be estimated with a total uncertainty of ±3.9%. For the background events with the third lepton in the forward region, the uncertainty is estimated to be ±10.7%. Assuming an integrated luminosity of 30 fb^{-1}, the total error on the WZ background can therefore be estimated to be ±7.8%. For an integrated luminosity of 100 fb^{-1}, this number is slightly reduced to ±7.1%.

4.3 Normalization of the WW and $t\bar{t}$ backgrounds

The remaining non resonant WW and $t\bar{t}$ backgrounds can be determined from the sidebands of the invariant di-lepton mass distribution. In Fig. 5 this distribution is shown after the selection criteria except the invariant Z mass cut are applied. The non resonant background below the peak can be determined from a fit of a Gaussian signal on top of the background. If data corresponding to an integrated luminosity of 30 fb^{-1} (100 fb^{-1}) are available an accuracy of ±6.4% (±3.5%) can be achieved.

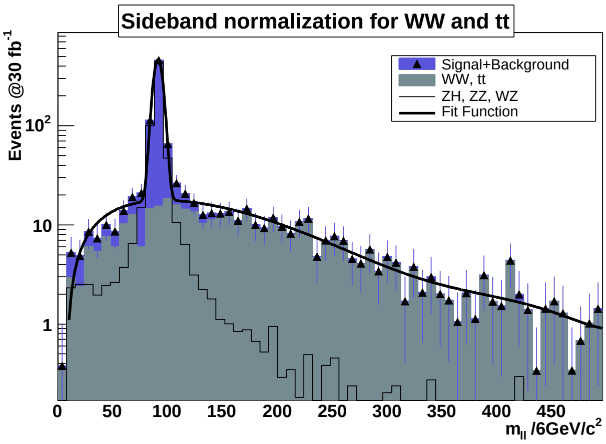

Figure 5: *Invariant mass of the di-lepton system for events passing all selection criteria except the invariant Z mass cut. A fit of a Gaussian signal on top of a relatively flat background is superimposed.*

5 Evaluation of the Signal Significance

The signal significance S can be evaluated using the number of signal and background events (N_S and N_B) and the systematic uncertainties on the background:

$$S = \frac{N_S}{\sqrt{N_B + (\alpha N_B)^2}} \tag{1}$$

In this equation α represents the relative systematic uncertainty on the total background and is calculated from the three background sources with their respective relative uncertainties α_i using standard error propagation:

$$\alpha = \frac{\sqrt{(\alpha^{ZZ} N_{ZZ})^2 + (\alpha^{WZ} N_{WZ})^2 + (\alpha^{WWtt} N_{WWtt})^2}}{N_B} \tag{2}$$

The results for the various relative errors are summarized in Table 9 for integrated luminosities of 30 and 100 fb^{-1}. The number of expected signal and background events and the

Background source	α(ZZ)	α(WZ)	α(WW and $t\bar{t}$)	combined α
30 fb^{-1}	8.5%	7.8%	6.4%	6.1%
100 fb^{-1}	4.9%	7.1%	3.5%	3.8%

Table 9: *Relative systematic uncertainties for the various background contributions and for the total background.*

calculated significance values for a Higgs boson discovery are summarized in Table 10 as a function of the Higgs boson mass. In addition to the significance a 95% confidence upper limit on the value of ξ^2, has been calculated. This value, defined as

$$\xi^2 \; = \; \mathrm{BR(H \to inv.)} \, \frac{\sigma_{\mathrm{ZH}}^{\mathrm{BSM}}}{\sigma_{\mathrm{ZH}}^{\mathrm{SM}}} \tag{3}$$

takes into account that a non-Standard Model Higgs boson might be produced with a different cross section as a Standard Model Higgs boson. If the production cross section is equal to the Standard Model one, ξ^2_{95} gives directly the branching ratio of the Higgs boson into invisible decays which can be excluded with a confidence level (C.L.) of 95%.

L (fb^{-1})	m_H (GeV/c^2)	120	140	160	180	200	300	400
30	N_S	126	98.7	73.5	54.9	41.7	9.9	2.1
	N_B				472.5			
	Significance S (w.o. syst.)	5.86	4.58	3.41	2.55	1.93	0.46	0.10
	Significance S	3.52	2.75	2.05	1.53	1.16	0.28	0.06
	ξ^2_{95}	0.47	0.60	0.81	1.08	1.42	5.99	28.2
100	Significance S	5.89	4.6	3.43	2.56	1.94	0.46	0.10
	ξ^2_{95}	0.28	0.36	0.48	0.64	0.85	3.57	16.9

Table 10: *Number of expected signal and background events, the discovery significance and the 95% C.L. upper limit on the variable ξ^2 (see text) for an integrated luminosity of 30* fb^{-1}*. The significance and ξ^2_{95} values are also given for an integrated luminosity of 100* fb^{-1}*.*

From the results obtained, it can be concluded that the detection of an invisibly decaying Higgs boson in the ZH channel at the LHC is difficult. For data corresponding to an integrated luminosity of 30 fb^{-1}, no discovery with a significance exceeding 5σ can be obtained if systematic uncertainties on the background are taken into account. For an integrated luminosity of 100 fb^{-1}, a discovery would be possible in the mass range up to 125 GeV/c^2. Assuming Standard-Model like production cross sections and totally invisible decays, BR ($H \to$ inv) = 100%, a 95% confidence level exclusion is possible over the mass range up to 170 GeV/c^2 and 250 GeV/c^2 for data corresponding to integrated luminosities of 30 and 100 fb^{-1} respectively. The corresponding 95% confidence level exclusion for the variable ξ^2_{95} is shown as a function of the Higgs boson mass in Fig. 6.

6 Comparison with other analyses

Studies of searches for invisible Higgs boson decays have already been carried out within the ATLAS collaboration for the associated ttH [17, 27] and for the vector boson fusion mode qqH [16]. In addition, a first study of the associated ZH production has been presented in Ref. [18].

The results obtained in the study of the qqH associated production are more promising than those obtained here and in Ref. [18]. Although this study obtains a larger sensitivity than the ttH production from Ref. [17], it seems that there is still room for improvements in the ttH channel, which is currently under investigation by the author [27]. The obtained 95% confidence level exclusions are shown in Fig. 6(right) for the analysis presented here and for the analyses from Refs. [16, 27]. The largest sensitivity is found in the vector boson fusion mode, qqH, however, it must be stressed that so far it is not clear how well those events can be triggered in ATLAS. They would require either a low threshold two-jet plus $\not{p}_T$ trigger or a dedicated topological two-jet trigger with large rapidity separation. Despite the smaller discovery power, a search in the associated ZH channel is important to understand whether a possible excess of events with large missing transverse energy in the associated production channels originates from Higgs boson production. In all cases evidence for a signal will be extracted from an excess of events with large $\not{p}_T$ above the background. For a reliable measurement a normalization of the backgrounds in the experiment will be necessary. In the associated ZH and $t\bar{t}H$ production modes the expected signal cross sections are small, in the range of a few fb, and the normalization is affected by large uncertainties. However, those channels are nevertheless of interest since they can be reliably triggered, and in addition, the $t\bar{t}H$ channel does not rely on the vector boson coupling, which might be suppressed in certain scenarios. It should also be mentioned that all studies performed only consider backgrounds from Standard Model processes. The impact of non-Standard Model backgrounds, which might be present if Higgs bosons decay invisibly, remains to be studied.

The results found in the present study are in reasonable agreement with the results obtained in Ref. [18]. In general, a somewhat lower signal acceptance and a larger WZ background is found in the present analysis. A more conservative estimate of the systematic uncertainties on the background leads to a lower signal significance.

7 Conclusions

In the present note the potential of the ATLAS experiment for the search of an invisibly decaying Higgs boson in the associated ZH production mode has been studied. The Z boson is required to be detected in its leptonic decay mode $Z \rightarrow \ell\ell$. Evidence for a signal is extracted from an excess of events with large $\not{p}_T$ above the background. In order to get a reliable signal extraction, the background, which is dominated by di-boson production, needs to be normalized from data. Since the signal and the background normalization are affected by large statistical uncertaintes, the discovery potential in this channel is found to be weaker than in the associated ttH and qqH channels.

For data corresponding to an integrated luminosity of 100 fb^{-1}, a 5σ discovery would be possible in the mass range up to 125 GeV/c^2. Assuming Standard-Model like production cross sections and totally invisible decays, BR ($H \rightarrow$ inv) = 100%, a 95% confidence level exclusion is possible over the mass range up to 250 GeV/c^2.

References

[1] ATLAS Collaboration, *Detector and Physics Performance Technical Design Report*, CERN/LHCC/99-15 (1999).

[2] S. Abdullin et al., *Summary of the CMS potential for the Higgs boson discovery,* CMS NOTE 2003/033.

[3] H. Haber, D. Dicus, M. Drees and X. Tata, Phys. Rev. **D37** (1987) 1367;
J.F. Gunion and H.E. Haber, Nucl. Phys. **B307** (1988) 445;
K. Griest and H.E. Haber, Phys. Rev. **D37** (1988) 719;
A. Djouadi et al., Phys. Lett. **B376** (1996) 220;
A. Djouadi, P. Janot, J. Kalinowski and P.M. Zerwas, Phys. Lett. **B376** (1996) 220;
A. Djouadi and M. Drees, Phys. Lett. **B407** (1997) 243.

[4] G. Belanger et al., Nucl. Phys. **B581** (2000) 3;
G. Belanger et al., Phys. Lett. **B519** (2001) 93, hep-ph/0106275;
G. Belanger et al., J. High Energy Phys. **03** (2004) 12, hep-ph/0310037.

[5] R.E. Shrock and M. Suzuki, Phys. Lett. **B10** (1982) 250;
L.F. Li, Y. Liu and L. Wolfenstein, Phys. Lett. **B159** (1985) 45.

[6] A.S. Joshipura and J.W.F. Valle, Nucl. Phys. **B397** (1993) 105.

[7] T. Binoth and J.J. van der Bij, Z. Phys. **C75** (1997) 17.

[8] N. Arkani-Hamed, S. Dimopoulos and G. Dvali, Phys. Lett. **B429** (1998) 263;
I. Antoniadis, N. Arkani-Hamed, S. Dimopoulos and G. Dvali, Phys. Lett. **B436** (1998) 257;
K. Dienes, E. Dudas and T. Gherghetta, Phys. Lett. **B436** (1998) 55 and Nucl. Phys. **B537** (1999) 47.

[9] S.P. Martin and D. Wells, Phys. Rev. **D60** (1999) 35006, hep-ph/9903259;
G.F. Giudice, R. Rattazzi and J.D. Wells, Nucl. Phys. **B595** (2001) 250, hep-ph/0002178.

[10] K. Belotsky et al., Phys. Rev. **D68** (2003) 054027, hep-ph/0210153.

[11] LEP Higgs boson working group, *Searches for invisible Higgs decays*, hep-ph/0107032;
DELPHI Collaboration, Eur. Phys. J. **C32** (2004) 475.

[12] D. Choudhury and D.P. Roy, Phys. Lett. **B322** (1994) 368, hep-ph/9312347;
S. Frederiksen, N. Johnson, G. Kane and J. Reid, Phys. Rev. **D50** (1994) 4244.

[13] J.F. Gunion, Phys. Rev. Lett. **72** (1994) 199, hep-ph/9309216.

[14] O.J.P. Eboli and D. Zeppenfeld, Phys. Lett. **B495** (2000) 147.

[15] H. Davoudiasl, T. Han and H.E. Logan, *Discovering an invisibly decaying Higgs at Hadron Colliders*, hep-ph/0412269.

[16] L. Neukermans and B. Di Girolamo, *Observing an invisibly decaying Higgs boson in ATLAS via vector boson fusion*, ATLAS note, ATL-PHYS-2003-006.

[17] B.P. Kersevan, M. Malawski and E. Richter-Was, Eur. Phys. J. **C29** (2003) 541.

[18] P. Gagnon, *Invisible Higgs boson decays in the ZH and WH channels*, ATL-PHYS-PUB-2005-011.

[19] F. Meisel, *Search for invisibly decaying Higgs bosons in SUSY scenarios in the ATLAS experiment*, diploma thesis, in preparation.

[20] R. Godbole et. al., *Search for invisible Higgs signals at the LHC via associated production with gauge bosons*, hep-ph/0304137.

[21] M. Spira, *h2hv program*, http://people.web.psi.ch/spira/v2hv

[22] H. Lai et. al, Eur. Phys. J. **C12** (2000) 375.

[23] B. Mellado et. al., *SM Higgs Production Cross-Sections and Branching Ratios for the ATLAS Higgs Working Group*, ATLAS Communication, ATL-COM-PHYS-2004-062.

[24] T. Sjostrand, Comp. Phys. Comm. **82** (1994) 74;
T. Sjöstrand, P. Eden, C. Friberg, L. Lönnblad, G. Miu, S. Mrenna and E. Norrbin, Comp. Phys. Comm. **135** (2001) 238, hep-ph/0010017.

[25] E. Richter-Was, D. Froidevaux and L. Poggioli, *ATLFAST, a fast simulation package for ATLAS*, ATLAS note, ATL-PHYS-98-131.

[26] D. Zeppenfeld, priv. communication.

[27] D. Schroff et al., *Study of the discovery potential of an invisibly decaying Higgs boson via the associated $t\bar{t}H$ production in the ATLAS experiment*, ATLAS note, in preparation.

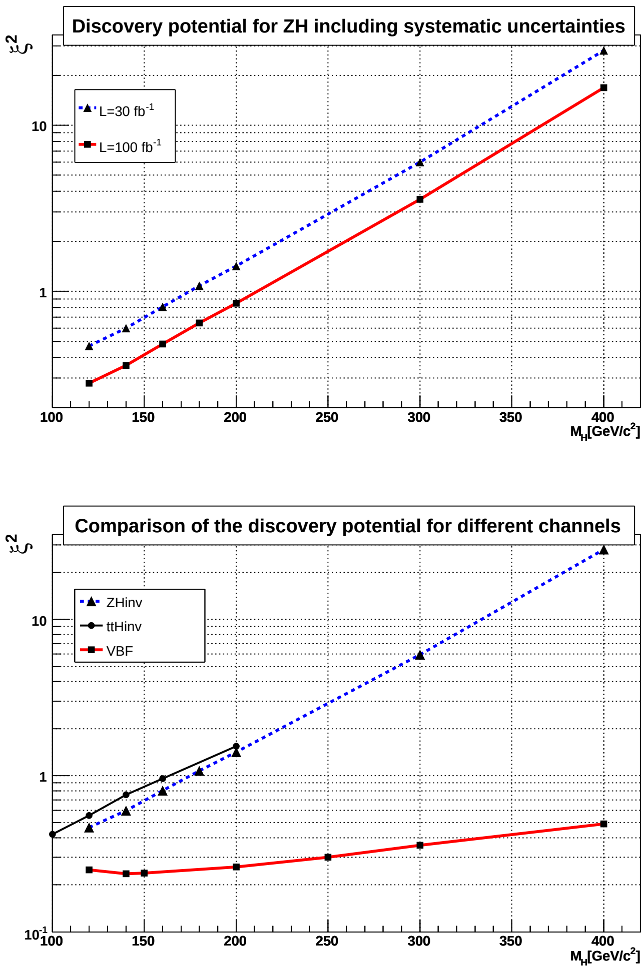

Figure 6: *Left: The 95% confidence level exclusion for the variable* ξ^2 *as obtained from a search for* ZH *production with* $Z \to \ell\ell$ *and* $H \to inv$ *(this analysis). Right: The 95% confidence level exclusion for the variable* ξ^2 *as obtained in the search for invisible Higgs boson decays in the* ZH*,* $t\bar{t}H$ *and* qqH *associated production assuming an integrated luminosity of 30* fb^{-1}.